

# A Study of Impurity-Free Vacancy Disordering in GaAs–AlGaAs for Improved Modeling

Amr Saher Helmy, *Student Member, IEEE*, N. P. Johnson, *Member, IEEE*, M. L. Ke, A. Catrina Bryce, *Member, IEEE*, J. Stewart Aitchison, *Member, IEEE*, John H. Marsh, *Senior Member, IEEE*, Ivair Gontijo, Gerald S. Buller, J. Davidson, and P. Dawson

**Abstract**—A study of the parameters of the process of impurity-free vacancy disordering (IFVD) of GaAs–AlGaAs quantum-well structures is presented. The study includes photoluminescence excitation measurements which show that the as-grown barrier/well interface is better fitted by an exponential profile than a square profile. This has a significant effect on the intermixed diffusion profiles. Also, deep level transient spectroscopy measurements have been conducted on samples that were processed using IFVD. The measurements show an elevated concentration of the trap EL2 in the processed samples, which is known to be related to As antisites. The concentration of such defects agrees with the concentration calculated for IFVD to within an order of magnitude, suggesting a correlation between the point defects required for IFVD and EL2. Finally, temporally and spatially resolved photoluminescence measurements were conducted on processed samples which indicate a factor of 3 reduction in the photogenerated carrier life time after undergoing IFVD. A spatial resolution better than 3  $\mu\text{m}$  has been observed.

**Index Terms**—Diffusion processes, optical spectroscopy, quantum heterostructures, quantum-well interdiffusion.

## I. INTRODUCTION

QUANTUM-WELL intermixing (QWI) is a technique by which the bandgap of a quantum confined heterostructure is selectively modified using postgrowth processing [1]. Amongst other applications [2], QWI is attractive as an alternative to regrowth and overgrowth processes [3], [4], which are the main techniques used in realizing optoelectronic and photonic integrated circuits (OEIC's and PIC's) [5]. Most research in the field to date has addressed technological aspects of the process, apart from a few exceptions where more microscopic characterization has been carried out [6], [7]. Achievements in characterization are lagging in comparison to technology due, partially, to the lack of a comprehensive

mathematical model of the processes involved in QWI, which, in turn, is a reflection of the depth of the studies undertaken [8]. Moreover, when characterising point defects, physical parameters are often inferred indirectly leaving room for much uncertainty and inaccuracy in the values obtained [9], [10]. Although some phenomenological quantitative models of QWI have been developed, they convey little about the process mechanisms and dynamics [11]. However, a quantitative analytical model has been reported recently [12], [13], whose accuracy is limited by the information available about the parameters associated with QWI. Although the reported model has succeeded in predicting the behavior of different QWI techniques, accurate determination of the parameters associated with each technique is crucial to the reliability of the model.

The processes studied in this work is impurity-free vacancy disordering (IFVD). IFVD uses group III vacancies introduced by the outdiffusion of Ga into dielectric caps at elevated temperatures to assist Ga–Al interdiffusion. The Ga outdiffusion leaves behind group III point defects (vacancies) in the semiconductor [14]. Since its discovery [15], IFVD has been utilized extensively to fabricate OEIC's and PIC's, due to its simplicity and the resulting low optical losses [3]. Due to the increasing use of IFVD in realising OEIC's and PIC's, the process parameters will be studied in more depth.

In this paper, we start by briefly describing the model which has been developed to explain QWI, and three limitations and approximations inherent in the model are highlighted. Experiments have been designed to address these limitations and the resulting data are then presented. The results of photoluminescence excitation (PLE) spectroscopy experiments are given, revealing interesting information about the interface abruptness of the as-grown quantum wells (QW's), as well as their diffusion profiles after IFVD. Deep level transient spectroscopy (DLTS) experiments are then reported, and specific deep level traps are related to the defects thought to contribute to IFVD. The DLTS measurements also reveal information about the concentration and diffusion of the defects with annealing duration and temperature. Spatially and temporally resolved photoluminescence studies have been performed on gratings fabricated using selective IFVD. The spatial resolution of the process as well as its effects on the carrier lifetimes in multiple-quantum-well (MQW) samples are deduced. These results are then analyzed and discussed leading to some conclusions about IFVD theory and technology.

Manuscript received January 28, 1998; revised May 18, 1998. The work of A. S. Helmy was supported by the Faculty of Engineering at the University of Glasgow and by the ORS award scheme in the U.K. This work was supported by the Engineering and Physical Sciences Research Council and the Ministry of Defence under Grant GR/K45968 and by the Engineering and Physical Sciences Research Council under Grant GR/L75467.

A. S. Helmy, N. P. Johnson, M. L. Ke, A. C. Bryce, J. S. Aitchison, and J. H. Marsh are with the Department of Electronics and Electrical Engineering, University of Glasgow, Glasgow G12 8QQ, Scotland, U.K.

I. Gontijo and G. S. Buller are with the Department of Physics, Heriot-Watt, Riccarton, Edinburgh EH 14 4AS, Scotland, U.K.

J. Davidson and P. Dawson are with the Department of Physics, University of Manchester Institute of Science and Technology, Manchester M60 1QD, U.K.

Publisher Item Identifier S 1077-260X(98)05856-0.

## II. ELEMENTS OF THE MODEL OF INTERMIXING KINETICS

In GaAs–AlGaAs heterostructures, compositional intermixing, and hence Al and Ga interdiffusion, is either carried out directly through diffusion of group III vacancies,  $V_{III}$ , or group III interstitials,  $I_{III}$  [6]. Regardless of the method by which the defects are introduced, during the annealing stage these defects will diffuse through the heterostructures. Any diffusion length that has been undertaken by a defect within the lattice is composed of a number of hops carried out in a random walk, as illustrated in Fig. 1. Within the regions in the lattice where  $[V_{III}]$  exceeds  $[I_{III}]$  as well as its equilibrium concentration, the movement of group III atoms is determined primarily by such vacancies. The model suggests that the transport of the Ga atoms during the interdiffusion occurs predominantly through  $V_{III}$ . Therefore, the diffusion coefficient of the Al/Ga in the barrier/well region is limited by the diffusion coefficient of the available vacancies,  $D_{vac}$ , and their number relative to the Ga concentration  $C_{Ga}$ .  $D_{Ga}$  can be written as

$$D_{Ga} = \left( \frac{N_v}{C_{Ga}} \right) D_{vac} \quad (1)$$

where  $N_v$  is the concentration of  $V_{III}$  at the QW/barrier interface. A more microscopic investigation shows that, at the interface of a heterostructure such as GaAs–AlAs QW's, each two crossings of the barrier/QW interface carried out by  $V_{III}$  will transport one Al atom one lattice hop toward the heterostructure. The total number of barrier/QW interface crossings undertaken by the atoms,  $N_{IC}$ , will therefore correspond to the entire number of lattice site-hops available for the Al–Ga interdiffusion, which can be calculated for a time span  $t$  from,

$$N_{IC} = \int_0^t \frac{w_v}{2} \cdot N_v(d_{QW}, t) \cdot dt \quad (2)$$

where  $N_v(d_{QW}, t)$  is the time dependent  $V_{III}$  concentration at the barrier/QW interface.  $N_{IC}$ , the total number of lattice hops available for group III interdiffusion predicted by the model, can therefore be calculated from the evolution of the defect profile with time  $N_v(d_{QW}, t)$ .

Although the model calculations were in good agreement with experimental results, one can clearly see that several approximations were used [16]. However, making the model more rigorous will not, in itself, result in better agreement with experiment because of other sources of inaccuracy, primarily:

- 1) The diffusion coefficient for Ga out-diffusion from the QW's is obtained by solving the Schrödinger equation for the bound states in the QW in conjunction with the diffusion equation, assuming diffusion of Ga in the semiconductor obeys Fick's law [16]. By using this approach, we disregard the effect of  $V_{III}$  on the Ga out-diffusion; an assumption which contradicts another one made earlier in the model stating the Ga out-diffusion takes place through  $V_{III}$ . Moreover, this assumption also leads to error function diffusion profiles, which impose concentrations for Ga and Al at the QW/barrier interface of  $C_o/2$  for small  $L_D$  [17]. Using PLE we will show that a better approximation to the true concentration profile can be inferred.

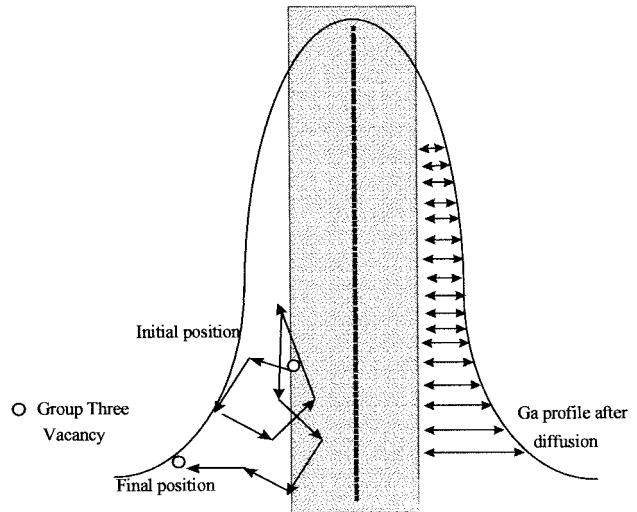


Fig. 1. Schematic diagram of the lattice hops involved in Ga out-diffusion from the quantum wells, with illustration of the random walk associated with group three vacancy diffusion.

- 2) The diffusion coefficient of  $V_{III}$  in GaAs–AlGaAs heterostructures has not yet been determined in an independent fashion. The two values quoted in the literature [9], [10] have been calculated in two different, but indirect, manners. The first was by monitoring the effects of  $V_{III}$  on charge density [9], and the second was determined by measuring the PL shifts produced in QWI, specifically IFVD [10]. Although the work reported in both papers involved reasonable justifications and approximations, considerable inaccuracy may exist in these numbers, due to the fact that the concentration profiles have been inferred indirectly. Both numbers agree to within a factor of 2 in the operating temperature range, namely 875 °C–950 °C. By using DLTS, the defect concentration can be measured.
- 3) An accurate knowledge of the actual spatial resolution of the IFVD processes should be developed so as to serve as a reference when the model is extended to two dimensions. By measuring spatially resolved PL and PL lifetime, we can obtain the spatial resolution of the process.

In the following sections of the paper, we shall investigate these points by carrying out the appropriate measurements for IFVD.

## III. EXPERIMENTAL STUDIES OF IFVD

### A. Photoluminescence Excitation Spectroscopy

PLE was used to determine the energies of the confined states in double quantum well (DQW) separate confinement heterostructure (SCH) p-i-n laser material. By studying the energies of the ground state as well as those of the higher confined states, and by fitting these measurements to an appropriate Al–Ga diffusion profile, an accurate estimate of the diffusion profile as a function of the annealing conditions can be deduced. As has been pointed out by Li *et al.* [18],

when only the lowest interband energy is used to characterize the intermixing process, errors are likely to occur.

The material used is described elsewhere [7]. The samples were cleaved up into square pieces of  $3 \times 3 \text{ mm}^2$ , and were coated with 200 nm of  $\text{SiO}_2$  deposited by electronic gun evaporation. The samples were then annealed, with the  $\text{SiO}_2$  caps present, at temperatures in the range  $875 \text{ }^\circ\text{C}$ – $950 \text{ }^\circ\text{C}$  for 60 s. PLE measurements were performed on a set of samples intermixed for different anneal temperatures along with one reference sample. A He–Ne laser was used for the PL measurement and a Ti:sapphire laser for PLE. The model and parameters used here are similar to those reported earlier [19], [20]. A conduction band offset of  $0.65\Delta E_g$  was used and band nonparabolicity was included as suggested by Ekenberg [21]. The electron band edge effective mass was taken to be  $0.0665m_0$ , while the Luttinger parameters as devised by Lawaetz were used to derive the heavy and light hole masses [22]. PL and PLE data obtained from three representative samples are shown in Fig. 2. From the PL data [Fig. 2(a)], it is obvious that the lowest band edge transition energy increases with increasing annealing temperature, which is also confirmed by the PLE data [Fig. 2(b)], where the lowest energy peak represents the excitonic transition between the lowest energy electron states and heavy hole states (e1-hh1). Many other transitions are also visible in the PLE spectra, which provide information on the behavior of the higher subbands with intermixing. Also clear from the spectra, is the decrease of the higher states' energies as the annealing temperature increases, which opposes the trend for the lowest two bound states. Another interesting result from the PLE data is that many of the observed transitions are in fact forbidden. It is well known that, under an ideal infinitely deep square well condition, only transitions with  $\Delta l = m - n = 0$ , where  $m$  and  $n$  are the subband indices of the conduction and valence bands respectively, are allowed because the wavefunctions of all other transitions are orthogonal. However, for a real QW which has a finite depth and may contain graded interfaces, the orthogonality of the wavefunctions is relaxed, resulting in a modified selection rule, where  $\Delta l \Rightarrow \text{even}$  transitions are allowed. This is why all possible transitions can be observed in absorption or excitation spectra [23].

The electronic band profile of the reference sample was initially calculated using a finite difference method, assuming a square well shape. Table I shows the various transition energies from both simulated and PLE data. While the two sets of data agree well for the lower transitions, there is, however, a noticeable discrepancy for the higher ones. Apparently, the calculated energies for the higher subbands are always larger than those observed experimentally, suggesting a wider well is needed for the higher subband. In order to take the behavior of the higher energy subbands into account, an exponential interface profile was used instead of the square well approximation. A well profile of the form

$$\begin{aligned} \zeta &= \zeta_0 \exp[-\beta/(z^2 - (L_w/2)^2)] \cdots |x| \geq L_w/2 \\ \zeta &= 0 \cdots |x| \leq L_w/2 \end{aligned} \quad (3)$$

was used, where  $\zeta$  is the energy profile of the well,  $\beta$  is the curvature parameter,  $L_w$  the initial well width (i.e., the width

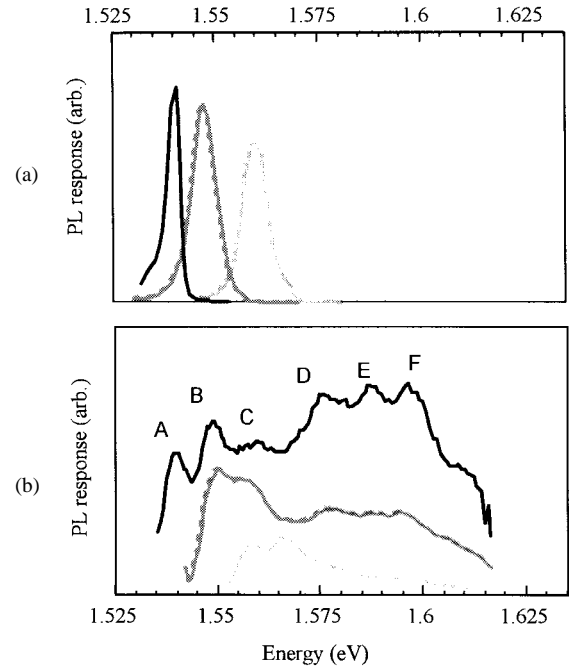


Fig. 2. Plot of (a) PL spectra of the samples used in the PLE experiment and (b) typical PLE spectra obtained from the samples.

TABLE I  
A STUDY OF IMPURITY-FREE VACANCY DISORDERING  
IN GaAs–AlGaAs FOR IMPROVED MODELING

Transitions	$E_{\text{measured}}$	$E_{\text{calculated}}$	
		Square well	Exponential well
E1-HH1 (A)	1.539 eV	1.541 eV	1.537 eV
E1-LH1 (B)	1.549 eV	1.551 eV	1.547 eV
E1-HH2 (C)	1.560 eV	1.563 eV	1.558 eV
E1-HH3 (D)	1.576 eV	1.586 eV	1.579 eV
E2-HH1 (D)	1.576 eV	1.587 eV	1.578 eV
E1-LH2 (E)	1.588 eV	1.604 eV	1.590 eV
E2-LH1 (E)	1.588 eV	1.602 eV	1.589 eV
E2-HH2 (F)	1.597 eV	1.616 eV	1.598 eV

of the bottom of the well). Using this profile a much better fit for all the transition energies was obtained as shown in Table I. Similar work has been reported recently indicating that an initial exponential profile for the QW's fits the measured data better than a square profile [24]. Error function profiles were also used to fit the data from the reference sample, but the calculated energies did not match the measured experimental data. The subband energies of the samples annealed at higher temperatures were fitted both to error function profiles and to Ga diffusion profiles resulting from an initial exponential QW profile, assuming a Fick's law diffusion. The latter fit leads to diffused quantum-well profiles described by the following equation,

$$\begin{aligned} C(z) &= \frac{C_0}{2\sqrt{\pi Dt}} \int_{(L_w/2)-z}^{\infty} \zeta(\eta) \cdot e^{-\eta/4Dt} d\eta \\ &+ \frac{C_0}{2\sqrt{\pi Dt}} \int_{(L_w/2)+z}^{\infty} \zeta(\eta) \cdot e^{-\eta/4Dt} d\eta \end{aligned} \quad (4)$$

where  $\zeta(\eta)$  is the initial exponential QW profile as given by

TABLE II  
A STUDY OF IMPURITY-FREE VACANCY DISORDERING  
IN GaAs–AlGaAs FOR IMPROVED MODELING

Transitions	$E_{\text{measured}}$	$E_{\text{calculated}}$	$L_D=8 \text{ \AA}$	$E_{\text{calculated}}$
	(eV)	Square well		(eV)
E1-HH1	1.549	1.549		1.546
E1-LH1	1.559	1.560		1.557
E1-HH2	1.567	1.574		1.566
E1-HH3	1.578	1.602		1.584
E2-HH1	1.578	1.603		1.585
E1-LH2	1.587	1.616		1.595
E2-LH1	1.587	1.615		1.596
E2-HH2	1.595	1.635		1.604

(3). The equation was solved numerically, and the energies of the diffused wells were obtained. As can be seen in Table II and Fig. 3, for an initial exponential profile with  $\beta = 500$  and subsequent diffusion, there is good agreement between experimental and calculated energy values of all of the transitions, not merely the ground level transition. As well as the profiles discussed, others were also studied including an initial *erfc* profile, which produced energy levels further away from the measured energies than those produced by the initial square well profile. Initial square wells with a thickness different than that specified during growth were also investigated giving rise to good fit for the lower energy level, e1-lh1, but inaccurate fit for the higher levels. In addition, asymmetric profiles were studied: results for single sided exponential profiles produced energy levels which fitted experimental results better than those produced by the square wells but not as good as those produced by the symmetric exponential profile, as can be seen in Fig 3. A QW profile with one side being an *erfc* profile and the other being an exponential profile was investigated giving rise to higher energy levels in good agreement with the measured ones, but the ground level, e1-lh1, was in poor agreement with the measured one. In brief, the symmetric exponential profile gave the best fit for the energy levels of both the initial QW and the interdiffused QW's. The QW diffusion behavior calculated for a square initial QW profile will obviously lead to errors in the obtained diffusion coefficients, which can be a considerable source of inaccuracy in the model.

### B. Deep-Level Transient Spectroscopy

The defects introduced during IFVD are known to be primarily  $V_{\text{III}}$  [6], [15]. Most of the evidence has been obtained from indirect measurements such as the Ga concentration in dielectric caps [25], [26], measurements of the Al–Ga interdiffusion coefficient during the annealing process [6], [9], etc. It would be an advantage to monitor the movement of such defects directly but, in general, the concentration and type of vacancy can be difficult to establish. A powerful method for characterising defects both in semiconductor material and in devices is DLTS [27]. This electrical method relies on shifting the depletion region edge through the depth of interest to fill the defect states, and then measuring the rate of emission of

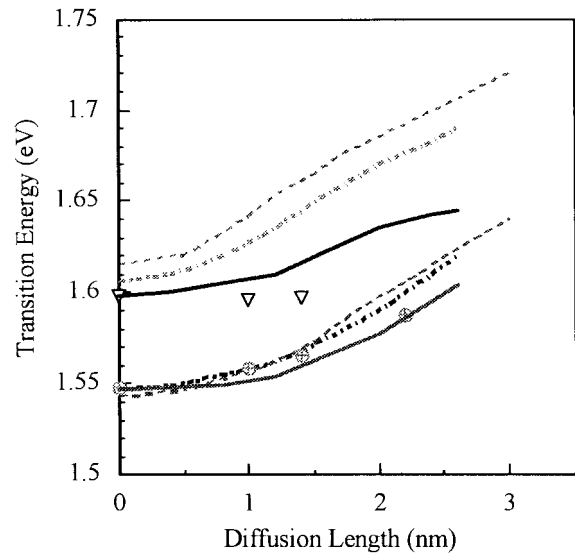


Fig. 3. Plot of the measured e1  $\rightarrow$  lh1, and e2  $\rightarrow$  hh2 transitions obtained from PLE measurements. Transitions fitted for an initial square, exponential, and single-sided exponential QW profiles are also plotted and represented by the dashed, solid, and dashed-dotted lines, respectively.

electrons and holes from the defects. Laser structures are not suitable for DLTS measurements as it is not possible to move the depletion region through the region of interest. In order to estimate the concentration of vacancies and other defects induced by the IFVD process, a  $p^+n$  junction was fabricated in GaAs to allow DLTS measurements.

The structure consisted of an  $n^+$ -substrate with a  $1.5\text{-}\mu\text{m}$   $n$ -type ( $2 \times 10^{16} \text{ cm}^{-3}$ ) layer, which is the minimum  $n$ -type background doping achievable with the machine used, capped by  $0.05 \mu\text{m}$  of  $p^+$  GaAs ( $6 \times 10^{18} \text{ cm}^{-3}$ ) grown by MOCVD. The reverse bias was varied between 0 and  $-5 \text{ V}$  so allowing the depth  $0.8\text{--}1.3 \mu\text{m}$  to be probed, leaving some margin for variation in doping concentration. The depths which could be probed are located at the same depths as the QW's in the SCH  $p\text{-i-n}$  laser structures [7]. Samples were cleaved to average dimensions of  $6 \times 6 \text{ mm}^2$  and were processed in exactly the same fashion as for the PLE samples. They were then patterned with four different diameter diodes after removing the  $\text{SiO}_2$  cap by wet etching using buffered HF for 30 s. P-type contacts were formed from Ti–Pd–Au with thicknesses of 33 nm/33 nm/150 nm, respectively, by evaporation and liftoff. N-type contacts were formed from Au–Ge–Au–Ni–Au with thicknesses of 11 nm/11 nm/14 nm/240 nm, respectively. Both contacts were annealed at  $360 \text{ }^\circ\text{C}$  for 60 s. The devices were then isolated by wet etching in a  $\text{H}_2\text{O}_2$ :Ammonia solution with a composition of 95:5 for 60 s using the p-contact as a mask, leading to a  $1\text{-}\mu\text{m}$  etch depth for isolation.

The reverse bias leakage current of the measured diodes was measured after fabrication. Some diodes from both processed and control samples showed large variations in leakage current. These were discounted, and only diodes falling on a straight line of leakage current versus diode area (confirming the absence of leakage from the edges) were wirebonded for measurement.

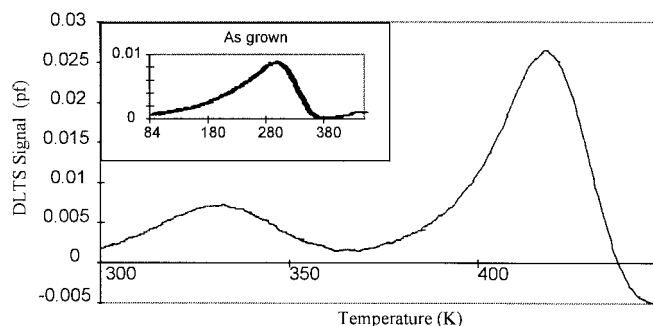


Fig. 4. Plot of the DLTS signal of a sampled annealed at 925 °C for 120 s.

On the as-grown sample, capacitance-voltage measurements indicate a doping concentration of around  $10^{16} \text{ cm}^{-3}$  at 0 V, which was confirmed using an electrochemical profiler, rising to  $10^{17} \text{ cm}^{-3}$  at  $-3.5 \text{ V}$ . This higher than expected doping gives a relatively small probe range of  $\sim 0.01 \mu\text{m}$  at a depth of  $\sim 1 \mu\text{m}$  depending on the particular doping for each sample. A comparison of results for the as-grown samples and for the same structure subjected to the IFVD process at 925 °C for 120 s is shown in Fig. 4. The as-grown sample has a relatively shallow level at 46 meV, which is native to the material. This may be the Si shallow donor at 58 meV, but with the emission energy influenced by field emission. The level is not detectable in the processed material and may be masked by the two induced deep levels shown in Fig. 4. The spectra were taken at a rate window of 1000/s with reverse bias of  $\sim 3.5 \text{ V}$  with a fill pulse duration of 3.8 ms. Arrhenius plots for several samples are shown in Fig. 5 which were obtained by varying the rate window over the range 1000/s to 0.8/s (the fill pulse width was also varied to match the measurement time). The variation in signature (activation energy and apparent cross section) has been confirmed as being due to the field dependence rather than sample variation. The closely identified levels EL2 and EL16 [28] are shown in Fig. 5 for comparison. The origin of EL2 has long been a source of controversy, though many authors agree that it is a complex involving an As antisite i.e. arsenic on a gallium site  $\text{As}_{\text{Ga}}$ , coupled to an arsenic interstitial  $\text{I}_{\text{As}}$  [29]. Phenomenologically, EL2 is found in bulk, VPE, and MOCVD material, and increases in concentration with As rich conditions. This is consistent with the out-diffusion of Ga into the  $\text{SiO}_2$  cap leaving As rich complexes behind associated with the excess Ga vacancies. An increase in the EL2 concentration has also been observed before for similar processing procedures [30]. EL16 is a trap also associated with VPE material although it has not been studied in much detail. Measurements at low reverse bias  $\sim 0.5 \text{ V}$  produce an added complication of sign reversal for the trap assigned EL2, which can lead to the trap being misinterpreted as a hole trap. This well known [29] artifact occurs when the series resistance is large compared with the capacitive reactance at the measurement frequency. The series resistance was independently measured on a HP LCR meter and found to be comparable to the capacitive reactance of the samples for samples showing sign reversal at low reverse bias, again confirmed by observation of the sign reversal from the 20/s rate window (normal electron trap)

to 50/s rate window (reversed, apparent hole trap) at 1-V reverse bias. The conclusion is that any hole like traps are merely artifacts of the high series resistance of the samples [31].

To obtain the trap concentration, the approximate formula,  $N_T = 2N_D \Delta C / C$  can be used. For  $N_D$  of  $3 \times 10^{17} \text{ cm}^{-3}$ , the formula gives a trap concentration value of  $N_T = 4 \times 10^{15} \text{ cm}^{-3}$  for EL2 and  $1.4 \times 10^{15} \text{ cm}^{-3}$  for EL16 for the sample annealed at 925 °C for 120 s. Broadly, it was found that the EL2 trap concentration increases with annealing temperature, though detailed analysis of the behavior with annealing temperature and time requires further investigation. The peak concentrations of the EL2 trap have been calculated and are plotted in Fig. 6. On the same graph, the defect concentrations calculated from the model are also plotted for the same anneal temperatures and at the same probing depth of  $1 \mu\text{m}$ . As can be seen, the order of magnitude agreement between the measured EL2 trap concentration and the defect concentration predicted by the model shows a strong correlation, except for the shortest anneal time of 30 s. This is thought to be due to numerical errors in the calculations occurring for short diffusion times [17]. Moreover, the nature of EL2, being known to represent As antisites, fits very well with the understanding of the IFVD process. The nonequilibrium group III vacancies, which are thought to be introduced by IFVD, will tend to attract any interstitial As atoms in the lattice, and form As antisites.

### C. Temporally and Spatially Resolved Photoluminescence

Temporally and spatially resolved PL measurements were used to investigate the spatial resolution of the intermixing process as well as the effect of intermixing on the photogenerated carrier lifetime. Samples were prepared with a grating field consisting of alternating intermixed/ nonintermixed stripes each  $8 \mu\text{m}$  wide. The intermixed/nonintermixed regions were covered by capping them with  $\text{SiO}_2$  and  $\text{SiO}_2\text{:P}$  respectively [32]. Two  $2 \times 2 \text{ mm}^2$  rectangular fields adjacent to the grating were also formed, one of which was capped with  $\text{SiO}_2$  and the other with  $\text{SiO}_2\text{:P}$  to produce test areas for CW PL studies. The sample was annealed 925 °C for 60 s. In Fig. 7, the 77 K CW PL spectra measured from the intermixed and nonintermixed areas adjacent to the grating are shown. A differential shift of  $\sim 30 \text{ nm}$  can be seen. Time and spatially resolved photoluminescence measurements were then performed on the grating.

A passively Q-switched semiconductor laser producing picosecond pulses of about 20-ps duration at a repetition rate of 1 MHz [33], was used as the excitation source, and a Si single-photon avalanche diode (Si-SPAD) was used for detection of the luminescence [34]. Besides the general advantages found in using solid-state devices when compared with photomultipliers, Si-SPAD's have a superior photon detection efficiency as well as a faster and undistorted time response [35], [36]. The small active area ( $\sim 7\text{-}\mu\text{m}$  diameter), is a considerable advantage in spatial resolution applications, giving a high spatial resolution with low sensitivity to spurious back scatter. The width of the instrumental response in the time domain in

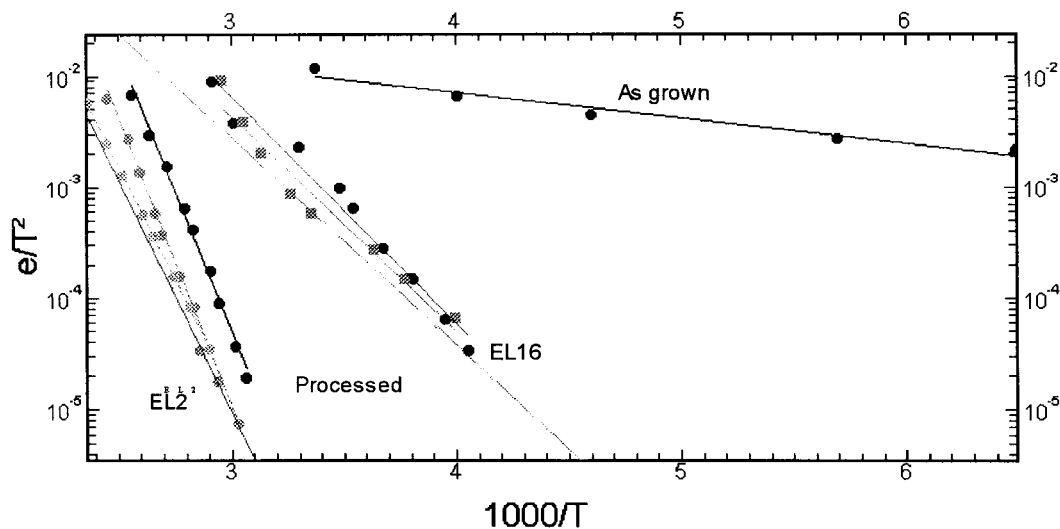


Fig. 5. Arrhenius plot of the signature of deep level traps identified in the various samples tested using DLTS.

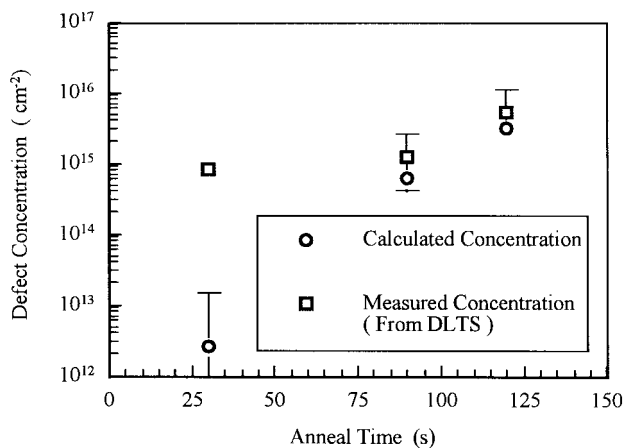


Fig. 6. Comparison of the number of point defects obtained from the DLTS measurements and those calculated from the model for the same annealing parameters.

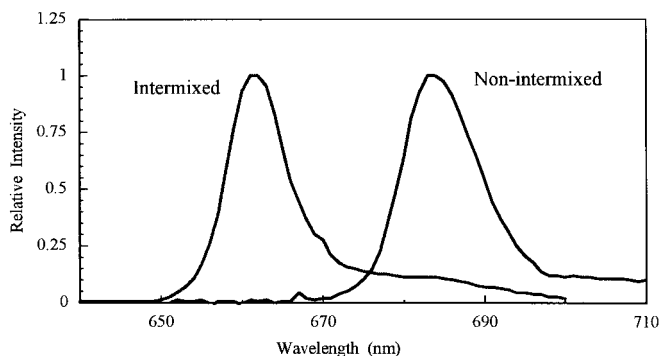


Fig. 7. PL spectra of the intermixed and nonintermixed regions, capped with  $\text{SiO}_2$  and  $\text{SiO}_2\text{:P}$ , respectively.

the system is around 80 ps (FWHM). The whole instrument is mounted on a microscope and has been described in detail elsewhere [37]. All measurements described below were performed at 77 K.

The wavelength of excitation was 677 nm and the laser was focused onto the sample, to a spot size of about  $2 \mu\text{m}$ .

PL was detected in the wavelength band  $690 \pm 5 \text{ nm}$ , which corresponds to the peak of emission of the nonintermixed material. Data were acquired for a fixed amount of time for each point of measurement, and these were linearly spaced by about  $1.5 \mu\text{m}$ . Once the PL decay times were measured, their FWHM, peak of emission and area (the integrated PL emission) could be calculated. In Fig. 8, the integrated PL and the decay time FWHM as functions of position are shown. The grating is clearly evident in both curves, having a period of approximately  $16 \mu\text{m}$ . It is interesting to see that the FWHM curve has maxima which are wider than its minima. This is an indication that the trap density responsible for the lifetime shortening has a strong lateral variation. The lifetime is minimum at the centre of the intermixed region and increases rapidly as the nonintermixed areas are approached. The integrated PL curve is more symmetrical, because the detection area is slightly larger than the laser spot size. Thus, PL photons generated by carriers that diffused from the excitation area could contribute to the total number of counts, but they would have markedly less effect on the decay times of the curves. The experimental PL decays were further analyzed by convolution of the instrumental response with an exponential function, to obtain the  $(1/e)$  decay times [38]. In general, the decays fitted well to single exponential functions, with time constants varying between 3 ns, for the nonintermixed regions, to approximately 1 ns, for the intermixed regions. The spatial resolution of the intermixing process can be estimated by taking it to be half of the distance between the 10%–90% points in the oscillations in Fig. 8. Using data from the FWHM results and from exponential fitting, the average spatial resolution and standard deviation obtained are 2.2 and  $0.6 \mu\text{m}$ , respectively. If, instead, data from both the spatially resolved integrated PL and peak PL are used, the values obtained are 3.0 and  $0.4 \mu\text{m}$ , respectively.

In the process of obtaining the estimates above, the effects of the laser spot size and finite detection area of the sample have not been taken into account. With a larger number of experimental points and knowing the laser spatial profile, it

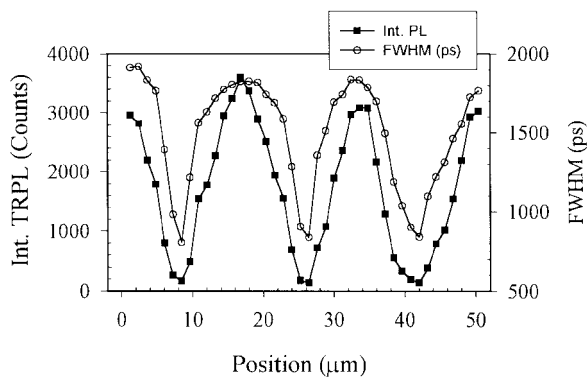


Fig. 8. Scan across a few periods of the grating for the PL signal detected at the excitonic peak of the nonintermixed section of the sample, and the photogenerated carrier life time.

should be possible to deconvolve the finite sizes of the laser spot and detected area from the measured results, to obtain the true spatial resolution. Therefore, the measurements above indicate that the spatial resolution of the intermixing process is better than  $3 \mu\text{m}$ , with the measurements being limited by the laser spot size. To the best of our knowledge, this is the highest spatial resolution measurement of QW intermixing processes using the TRPL technique. Previous measurements of QW's intermixed using a pulsed laser technique had established an upper limit of about  $20 \mu\text{m}$  for the spatial resolution of the process [39].

#### IV. CONCLUSION

We have presented the elements of a model describing the kinetics of intermixing of GaAs–AlGaAs quantum confined heterostructures. The approximations in the model were highlighted. The results from PLE measurements and the associated bound state calculations showed that the as-grown QW interfaces have exponential profiles rather than abrupt profiles. The corresponding diffusion profiles are therefore better fitted with profiles obtained by solving the diffusion equation with an exponential profile as an initial condition for the QW's. DLTS measurements showed that the dominant trap introduced by IFVD has an activation energy similar to that of EL2. This identification would be consistent with the understanding of the mechanisms of QWI through IFVD. Moreover, the measured trap densities were of the same order of magnitude as those calculated from the model. Future experiments designed to correlate the defects with the annealing conditions are in progress. Spatially resolved PL measurements show that the spatial resolution of IFVD for a  $1.5\text{-}\mu\text{m}$ -thick MQW layer located  $1 \mu\text{m}$  below the surface is of the order of  $2.2 \mu\text{m}$ , and is certainly better than  $3 \mu\text{m}$ . Time-resolved PL data show a factor of 3 reduction in the photogenerated carrier life time as intermixing takes place, confirming the presence of point defects.

#### ACKNOWLEDGMENT

One of the authors, A. S. Helmy, would like to thank B. S. Ooi and E. A. Avrutin for assistance.

#### REFERENCES

- [1] B. S. Ooi, K. McIlvaney, M. W. Street, A. Saher Helmy, S. G. Ayling, A. C. Bryce, J. H. Marsh, and J. S. Roberts, "Selective quantum-well intermixing in GaAs/AlGaAs structures using impurity-free vacancy diffusion," *IEEE J. Quantum Electron.*, vol. 33, pp. 1784–1793, 1997.
- [2] M. W. Street, N. D. Whitbread, D. C. Hutchings, J. M. Arnold, J. H. Marsh, J. S. Aitchison, G. T. Kennedy, and W. Sibbett, "Quantum-well intermixing for the control of second-order nonlinear effects in AlGaAs multiple-quantum-well waveguides," *Opt. Lett.*, vol. 22, pp. 1600–1602, 1997.
- [3] A. C. Bryce, F. Camacho, E. A. Avrutin, and J. H. Marsh, "CW and mode-locked integrated extended cavity lasers fabricated using impurity free vacancy disordering," *IEEE J. Quantum Electron.*, vol. 33, pp. 1784–1793, 1997.
- [4] P. J. Poole, M. Davies, M. Dion, Y. Feng, S. Charbonneau, R. D. Goldberg, and I. V. Mitchell, "The fabrication of a broad-spectrum light-emitting diode using high-energy ion-implantation," *IEEE Photon. Technol. Lett.*, vol. 8, pp. 1145–1147, 1996.
- [5] J. E. Zuker, K. L. Jones, M. A. Newkirk, R. P. Gnall, B. I. Miller, M. G. Young, U. Koren, C. A. Burrus, and B. Tell, "Quantum well interferometric modulator monolithically integrated with 1.55 mm tunable distributed Bragg reflector laser," *Electron. Lett.*, vol. 28, pp. 1888–1889, 1992.
- [6] D. G. Deppe and N. Holonyak, Jr., "Atom diffusion and impurity induced layer disordering in quantum well III–V semiconductor heterostructures," *Appl. Phys. Lett.*, vol. 64, pp. R93–R113, 1988.
- [7] I. Gontijo, T. Krauss, J. H. Marsh, and R. M. De La Rue, "Postgrowth control of GaAs/AlGaAs quantum-well shapes by impurity-free vacancy diffusion," *IEEE J. Quantum Electron.*, vol. 30, pp. 1189–1195, 1994.
- [8] Y. T. Oh, T. W. Kang, C. Y. Hong, K. T. Kim, and T. W. Kim, "The relation between Ga vacancy concentrations and diffusion lengths in intermixed GaAs/Al<sub>0.35</sub>Ga<sub>0.65</sub>As multiple-quantum wells," *Solid State Commun.*, vol. 96, pp. 241–244, 1995.
- [9] K. B. Kahen D. L. Peterson, G. Rajeswaran, and D. J. Lawrence, "Properties of Ga vacancies in AlGaAs materials," *Appl. Phys. Lett.*, vol. 55, pp. 651–653, 1989.
- [10] S. Y. Chiang and G. L. Pearson, "Properties of vacancy defects in GaAs single crystals," *J. Appl. Phys.*, vol. 46, pp. 2986–2991, 1975.
- [11] W. P. Gillin, A. C. Kimber, D. J. Dunstan, and R. P. Webb, "Diffusion of ion-beam created vacancies and their effect on intermixing—A gambler's ruin approach," *J. Appl. Phys.*, vol. 76, pp. 3367–3371, 1994.
- [12] A. S. Helmy, J. S. Aitchison, and J. H. Marsh, "The kinetics of intermixing of GaAs/AlGaAs quantum confined heterostructures," *Appl. Phys. Lett.*, 1997, pp. 2998–3000.
- [13] ———, "The kinetics of intermixing of GaAs/AlGaAs quantum confined heterostructures," in *LEOS 10th Annu. Meet.*, 1997, pp. 445–446, paper ThT1.
- [14] K. V. Vaidyanathan, M. J. Helix, D. J. Wolfrod, B. G. Streetman, R. J. Blattner, and C. A. Evans Jr., "Study of Encapsulants for annealing GaAs," *J. Electrochem. Soc.*, vol. 124, pp. 1781–1784, 1977.
- [15] D. G. Deppe, L. J. Guido, N. Holonyak, Jr., K. C. Hsieh, R. D. Burnham, R. L. Thorton, and T. L. Paoli, "Stripe-geometry quantum well heterostructure Al<sub>x</sub>Ga<sub>1-x</sub>As-GaAs lasers defined by defect diffusion," *Appl. Phys. Lett.*, vol. 49, pp. 510–512, 1986.
- [16] J. R. Manning, *Diffusion Kinetics for Atoms in Crystals*. Princeton, NJ: Van Nostrand, 1968.
- [17] A. S. Helmy, J. S. Aitchison, and J. H. Marsh, "Quantitative model for the kinetics of compositional intermixing in GaAs/AlGaAs quantum confined heterostructures," *IEEE J. Quantum Electron.*, submitted for publication.
- [18] E. H. Li, B. L. Weiss, and K. S. Chan, "Effect of interdiffusion on the subbands in an AlGaAs/GaAs single QW structure," *Phys. Rev. B*, vol. 46, pp. 15181–15192, 1992.
- [19] M. L. Ke and B. Hamilton, "Electronic structure of  $\delta$ -doped quantum wells," *Phys. Rev. B*, vol. 47, pp. 4790–4793, 1993.
- [20] M. L. Ke, J. S. Rimmer, B. Hamilton, J. A. Evans, M. Missous, K. E. Singer, and P. Zalm, "Radiative transitions associated with hole confinement at Si delta doped planes in GaAs," *Phys. Rev. B*, vol. 45, pp. 14114–14117, 1992.
- [21] U. Ekenberg, "Enhancement of nonparabolicity effects in a quantum well," *Phys. Rev. B*, vol. 36, pp. 6152–6155, 1987.
- [22] P. Lawaetz, "Valence-band parameters in cubic semiconductors," *Phys. Rev. B*, vol. 4, pp. 3460–3467, 1971.
- [23] W. T. Masselink, P. J. Pearah, J. Klem, C. K. Peng, H. Morkoc, G. D. Sanders, and Y. C. Chang, "Absorption coefficients and exciton oscillator strength in AlGaAs/GaAs superlattices," *Phys. Rev. B*, vol. 32, pp. 8027–8034, 1985.

- [24] W. C. H. Choy, P. J. Hughies, and B. L. Weiss, "The confinement profile of As-grown MOVPE AlGaAs/GaAs quantum well structures," *Mater. Res. Soc. Symp. Proc.*, vol. 450, pp. 425–430, 1997.
- [25] X. Wen, J. Y. Chi, E. S. Koteles, B. Elman, and P. Melman, "Processing parameters for selective intermixing of GaAs/AlGaAs quantum wells," *J. Electron. Mater.*, vol. 19, pp. 539–542, 1990.
- [26] T. Haga, N. Tachino, Y. Abe, J. Kasahara, A. Okubora, and H. Hasegawa, "Out-Diffusion of Ga and As atoms into dielectric films in SiO<sub>x</sub>/GaAs and SiNy/GaAs systems," *J. Appl. Phys.*, vol. 66, pp. 5809–5815, 1989.
- [27] D. V. Lang, "Deep level transient spectroscopy: A new method to characterize traps in semiconductors," *J. Appl. Phys.*, vol. 45, pp. 3023–3033, 1974.
- [28] G. M. Martin, A. Mitonneau, and A. Mircea, "Electron traps in bulk and epitaxial GaAs crystals," *Electron. Lett.*, vol. 13, pp. 191–192, 1977.
- [29] J. C. Bourgoin, H. J. von Bardeleben, and D. Stievenard, "Native defects in gallium arsenide," *J. Appl. Phys.*, vol. 64, pp. R65–R91, 1988.
- [30] F. Hasegawa, N. Yamamoto, and Y. Nannichi, "Change of the surface density of the midgap level (EL2 or EL0) in bulk GaAs by heat treatment with various capping," *Appl. Phys. Lett.*, vol. 45, pp. 461–463, 1984.
- [31] D. K. Schroder, *Semiconductor Material and Devices Characterization*. New York: Wiley, 1990.
- [32] P. Cusumano, B. S. Ooi, A. S. Helmy, S. G. Ayling, A. C. Bryce, J. H. Marsh, B. Voegelé, and M. J. Rose, "Suppression of quantum well intermixing in GaAs/AlGaAs laser structures using phosphorus-doped SiO<sub>2</sub> encapsulant layers," *J. Appl. Phys.*, vol. 81, pp. 2445–2447, 1997.
- [33] E. L. Portnoi, N. M. Stel'makh, and A. V. Chelnokov, "Characteristics of heterostructure lasers with a saturable absorber fabricated by deep ion implantation," *Sov. Tech. Phys. Lett. (USA)*, vol. 15, pp. 432–433, 1989. Transl. of: *Pis'ma v Zh. Tekh. Fiz.* (U.S.S.R.).
- [34] S. Cova, M. Ghioni, A. Lacaita, C. Samori, and F. Zappa, "Avalanche photodiodes and quenching circuits for single-photon detection," *Appl. Opt.*, vol. 35, pp. 1956–1976, 1996.
- [35] A. Lacaita, M. Ghioni, and S. Cova, "Double epitaxy improves single-photon avalanche diode performance," *Electron. Lett.*, vol. 25, pp. 841–843, 1989.
- [36] S. Cova, A. Lacaita, M. Ghioni, G. Ripamonti, and T. A. Louis, "20 ps timing resolution with single photon avalanche diodes," *Rev. Sci. Instrum.*, vol. 60, pp. 1104–1110, 1989.
- [37] G. S. Buller, J. S. Massa, and A. C. Walker, "All-solid-state microscope-based system for picosecond time-resolved photoluminescence measurements on II-VI semiconductors," *Rev. Sci. Instrum.*, vol. 63, pp. 2994–2998, 1992.
- [38] D. V. O'Connor and D. Phillips, *Time-Correlated Single Photon Counting*. New York: Academic, 1983.
- [39] S. J. Fancey, G. S. Buller, J. S. Massa, A. C. Walker, C. J. McLean, A. McKee, A. C. Bryce, J. H. Marsh, and R. M. De La Rue, "Time-resolved photoluminescence microscopy of GaInAs/GaInAsP quantum wells intermixed using a pulsed laser technique," *J. Appl. Phys.*, vol. 79, pp. 9390–9392, 1996.

**Amr Saher Helmy** (S'94), for a biography, see this issue, p. 660.

**N. P. Johnson** (M'96), photograph and biography not available at the time of publication.

**M. L. Ke**, photograph and biography not available at the time of publication.

**A. Catrina Bryce** (M'91), for a biography, see this issue, p. 646.

**J. Stewart Aitchison** (M'96), for a biography, see this issue, p. 660.

**John H. Marsh** (M'91–SM'91), for photograph and biography, see this issue, p. 583.

**Ivair Gontijo** was born in Minas Gerais, Brazil, in 1960. He received the B.Sc. degree in physics and the M.Sc. degree in optics and crystal growth from the Universidade Federal de Minas Gerais, Brazil, in 1985 and 1987, respectively, and the Ph.D. degree from the University of Glasgow, U.K., in 1992.

While in Brazil, he worked on the growth of organic crystals and performed dynamic light scattering experiments at the crystal-melt interface. At the University of Glasgow, he worked on the fabrication and picosecond optical characterization of semiconductor devices, including Auston switches, coplanar waveguides, and MESFET's. Then, at the same university, he joined the Optoelectronics group as a Research Assistant, to work on the demonstration of a high-speed all-optical clock-recovery system and also on the physics and technology of quantum-well intermixing. In 1994, he joined the Physics Department at Heriot-Watt University, Edinburgh, Scotland, U.K., as a Research Associate, working first with resonant optical nonlinearities in InP-based waveguides and then on the development of III-V single-photon avalanche photodiodes for time-resolved photoluminescence measurements up to 1.6  $\mu\text{m}$ . He is now with the Department of Electrical Engineering Department, University of California at Los Angeles. His main research interests include optoelectronics in general and lasers, waveguides, modulators, and detectors.

Dr. Gontijo is a member of the Optical Society of America.

**Gerald S. Buller** was born in Glasgow, Scotland, U.K., on January 16, 1965. He received the B.Sc. degree in natural philosophy from the University of Glasgow, Glasgow, Scotland, U.K., in 1986 and the Ph.D. degree in physics from Heriot-Watt University, Edinburgh, Scotland, U.K., in 1989.

He has been a Lecturer in the Department of Physics, Heriot-Watt University since 1990. His research interests mainly concentrate in applications of photon-counting technology, including time-resolved photoluminescence and time-of-flight optical ranging, specifically in the use of semiconductor single-photon avalanche diodes at infrared wavelengths, up to and including 1.55  $\mu\text{m}$ . His other research interests include optical thin-film multilayer coatings, particularly the design, growth and characterisation of structures grown by ion-assisted deposition.

**J. Davidson**, photograph and biography not available at the time of publication.

**P. Dawson**, photograph and biography not available at the time of publication.